Further Considerations for Approximating a Physics-Based Model of Surface Reflection Loss

Adrian David JONES; Alex ZINOVIEV; David Wayne BARTEL

Defence Science and Technology Organisation, Australia

ABSTRACT

Previously, the authors prepared a model of the coherent acoustic reflection loss at the ocean surface by combining an existing model of roughness loss with a description of surface grazing angle which accounted for the near-surface sound speed reductions due to an assumed distribution of wind-driven bubbles. More recently, the authors showed that the full derivation of surface incidence angle, which was based on an analysis by Brekhovskikh, could be approximated by a simple expression in terms of the physical parameters of the assumed model of bubble population, together with wind speed and frequency. In an extension to this work, the practical limits to the application of this approximated solution are examined, in terms of the wind speed-frequency combinations, and the range of grazing angles, for which it is adequate. The adequacy of the approximated model is tested by incorporating it within a Gaussian-beam acoustic propagation code and generating loss values for surface ducted transmission scenarios, to compare against data obtained by Monte Carlo runs of Parabolic Equation (PE) transmission calculations for which the sea surface is roughened and the near-surface sound speed reductions from the bubble distribution are included.

Keywords: Underwater Sound, Ocean, Surface Reflection
I-INCE Classification of Subjects Number(s): 54.3

1. INTRODUCTION

The propagation of sound in a mixed layer surface duct may be affected significantly by a wind-roughened ocean surface. Due to the roughness, acoustic energy can be scattered in non-specular directions thus causing a reflection loss. Near surface bubbles generated by the wind may change the sound speed, and may be a direct cause of sound scattering and absorption. As a result, the condition of the ocean surface must be taken into consideration in any realistic model of sound propagation within the surface duct. In the work of this paper, the acoustic frequencies are assumed sufficiently low that bubble scattering and absorption may be neglected.

Existing models of surface reflection loss usually take the grazing angle at the ocean surface as an input parameter, and usually this angle is computed from sound speed using Snell’s law. However, in situations where the sound speed change is considerable on the scale of the acoustic wavelength, Snell’s law is not necessarily applicable and a wave-based theory becomes necessary. The presence of wind-induced air bubbles in the ocean near the surface may cause significant reduction of the sound speed near the surface and so an improved model is required.

Jones et al. (1) suggested a model for evaluating the loss of acoustic energy due to reflection from the wind-roughened ocean surface. The model was called “JBZ” by the authors and is based on combining a model of surface roughness loss with a novel method of evaluating the grazing angle at the surface. The determination of surface angle uses a solution of the wave equation in a vertically stratified layer as formulated by Brekhovskikh (2) for a “transitional layer” between two media with different values of the equilibrium sound speed. The sound speed variation assumed in the bubbly region in the ocean, which needs to be matched to an example of “transitional layer”, uses the model described by Ainslie (3), which in turn uses the Hall-Novarini bubble population model (Hall (4), Keiffer et al. (5)). This solution for surface angle has been considered in detail by Zinoviev et al (6) who demonstrated that, if the incident grazing angle at the bottom of the bubbly layer is of the order of a few degrees or less, as will be the case for ducted transmission, the grazing angle at the surface may differ significantly from the value predicted by Snell’s law.

The suitability of using the JBZ model of coherent surface reflection loss with a model of sound transmission was successfully demonstrated by Jones et al. (7). In the original JBZ model, the computation of the grazing angle at the surface contains a slowly converging infinite series and depends on parameters of the layer which need to be obtained from numerical matching the sound speed profile in the real layer and the transitional layer described by Brekhovskikh (2). Therefore, to make the wave-based method of calculating the grazing angle at the surface more practicable, its theoretical formulation needed to be simplified.

This paper describes an approximate solution for the grazing angle at the surface. An approximation for the surface roughness loss is also presented, and the two are combined to create a "simplified JBZ" model. Lastly, *TL* results are shown from the use of the simplified JBZ model with a Gaussian beam transmission model, for a surface ducted scenario, in comparison with results obtained using a PE code. This paper extends a recent presentation of progress in this work (8) to consider the practical limits to the application of the simplified JBZ model, in terms of the wind speed-frequency combinations, and the range of grazing angles, for which it is adequate.

2. SURFACE ROUGHNESS LOSS FUNCTION APPROXIMATION

In earlier work involving the authors (1), it was shown that the coherent Reflection Loss (*RL*) in dB per surface reflection, obtained from the second-order small-slope approximation (SSA) method as used and described by Williams et al. (9) can be adequately approximated as a linear function in surface grazing angle β_s for small angles, and by the Kirchhoff (KA) model of reflection loss for the surface grazing angles for which the Kirchhoff loss exceeds the linear approximation. The expressions of loss for the linear approximation and KA model are as follows:

$$RL \approx 2.79\times10^{-7} f^{3/2}\left(w_{19.5}\right)^3 \beta_s \quad \text{linear approximation for small } \beta_s \tag{1}$$

$$RL \approx 0.019\left[f\left(w_{19.5}\right)^2 \sin\beta_s / c_s\right]^2 \quad \text{for KA model} \tag{2}$$

where surface grazing angle β_s is in radians; *f* is cyclic frequency, Hz; c_s is speed of sound in bubble-free seawater at ocean surface, m/s; $w_{19.5}$ is wind speed, m/s, and an example application is shown in Figure 1.

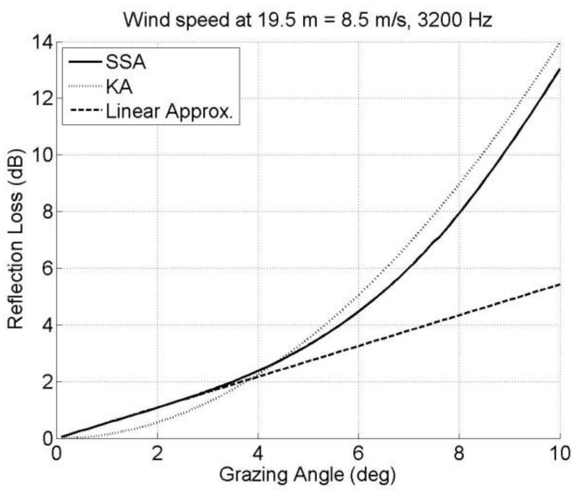

Figure 1 – Coherent Reflection Loss per bounce, 8.5 m/s wind speed $w_{19.5}$, 3200 Hz

With the full JBZ model in use with a ray model, an angle of surface incidence, determined by neglecting the bubble effects, is presumed to be the same as the angle of incidence β_0 immediately below the bubbly region. This angle is input to an analysis based on the Brekhovskikh "transitional layer" to determine a revised value of surface angle β_s for input to the SSA model to determine the loss in dB to be applied. The simplified JBZ model is similar, but the surface incidence angle β_s is obtained using an approximation to the full analysis based on Brekhovskikh's transitional layer, and then the greater of the loss values from Equations (1) and (2) is the loss value used in the ray model.

3. SOUND SPEED PROFILE IN THE SURFACE BUBBLE LAYER

As shown by Zinoviev et al. (6), the sound speed profile in the "transitional layer" described by Brekhovskikh (2) is expressed in terms the vertical coordinate, z, which is zero at the ocean surface and positive with depth. If the sound speed far below the surface is c_0, the profile of the transitional layer can be determined by the following equation:

$$c(z) = c_0 \sqrt{\frac{1-N}{1-N\left[\dfrac{e^{mz}}{1+e^{mz}}\right]}}, \quad z > 0. \tag{3}$$

In Equation (3), N and m are parameters of the layer. Setting z = 0, N follows as

$$N = 1 - \left(c_s^{\,2} / \left[2c_0^{\,2} - c_s^{\,2}\right]\right) \tag{4}$$

where $c_s = c(0)$ is the sound speed at the surface, and N is non-dimensional.

In the application to the bubbly region near the ocean surface, the speed of sound c_0 is the value existing below the bubbly region. The nature of N and m may be more easily understood with reference to Figure 2. Here, the variations in sound speed in the vicinity of the surface may be seen in their dependence on N and m. In Figure 2(a), N may be seen to represent the (non-dimensional) magnitude of the sound speed variation in the layer (the "strength" of the layer), and for the application to the wind-driven bubbly layer in the ocean, values are much less than 1. In Figure 2(b), m may be seen to represent the thickness of the layer. From Equation (3), m has dimensions of m^{-1}. A value of m = 0 corresponds to an infinitely wide layer, whereas at $m \to \infty$ the layer is infinitely thin.

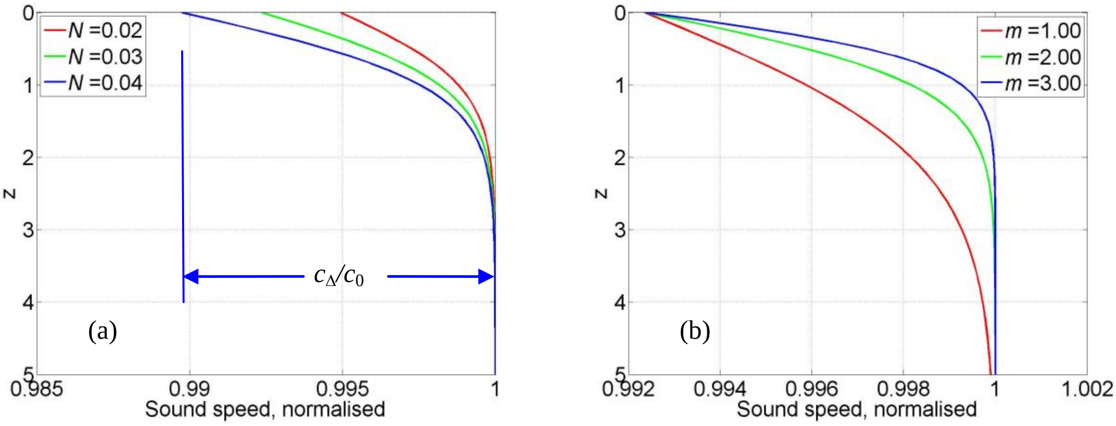

Figure 2 – Normalised sound speed profiles for transitional layer for (a) different values N, m = 2, (b) different values of m, N = 0.03

If the change in surface sound speed caused by the bubbles, $c_0 - c_s = c_\Delta$, is small relative to c_0, as will always be the case, the strength of the layer N may be approximated as

$$N \approx 4c_\Delta / c_0 \tag{5}$$

where c_Δ is regarded as positive when the sound speed is reduced by the bubbles.

3.1 Determination of layer "strength" *N* from physical parameters

In an earlier formulation of this work, Zinoviev et al. (6) devised a numerical matching process by which the value of N was determined from the application of Equation (4) to sound speed data obtained using the analysis of bubble population and sound speed presented by Ainslie (3). Subsequently, it was considered preferable to relate N directly to the parameters of the model of bubble population. This new analysis is described below.

For the wind-driven bubble layer, sound speed values are modified as (after Ainslie's Equation 14)

$$\left[\frac{c_0}{c(z)}\right]^2 = 1 + \frac{\rho_0 c_0^{\,2}}{\kappa(z)P(z)} U(z) \tag{6}$$

where c_0, in m/s, is the speed of sound in bubble-free seawater, and is assumed independent of depth as the change in sound speed due to the pressure effect (about 0.017 s^{-1}) may be considered negligible for relevant depths. In addition $c(z)$, in m/s, is the speed of sound in bubbly water at depth z; ρ_0 is the density of bubble-free seawater in kg/m^3 (assumed depth independent); $\kappa(z)$ is the polytropic index for the gas in bubbles at depth z (where $\kappa(z)$= 1.0 for isothermal compression and $\kappa(z)$= 1.4 for adiabatic compression – isothermal compression assumed in this analysis); $P(z)$ is the absolute hydrostatic pressure inclusive of atmospheric pressure, in Pa, at depth z; and $U(z)$ is the air fraction of seawater at depth z. Of course, $c(0)$ is the same as c_s.

By evaluating the necessary terms in Equation (6), a modified profile of sound speed values $c(z)$ is determined. It must be noted that Ainslie's analysis is in terms of a value of wind speed w_{10} relevant to 10 m height above sea level. In order to perform simulations at nominal wind speed values $w_{19.5}$, where those values are referenced to a height 19.5 m above sea level, the wind speed values input to Ainslie's analysis were modified by the proportion 0.94, to account for the relationship $w_{10} \approx 0.94 w_{19.5}$ that Ainslie attributed to Dobson. Ainslie's expression (3) for the air fraction of seawater at the surface, $U(0)$, using Novarini's modification of the bubble population model of M.V.Hall, then becomes

$$U(0) = 7.72 \times 10^{-10} (w_{19.5})^3 . \tag{7}$$

If Equation (6) is expressed in terms of surface values, for which z = 0, after some manipulation, and substitution of 1.0 for $\kappa(z)$ as has been assumed, the surface sound speed $c(0) = c_s$ is

$$c_s \approx c_0 - \frac{\rho_0 c_0^{\,3} U(0)}{2 P_0} \tag{8}$$

where P_0 is absolute hydrostatic pressure at ocean surface, Pa. Next, obtaining $c_0 - c_s = c_\Delta$ and substituting in Equation (5) gives

$$N \approx \frac{2 \rho_0 c_0^{\,2} U(0)}{P_0} . \tag{9}$$

Substituting for the air fraction at the surface using Equation (7), and for c_0 as 1500 m/s, ρ_0 as 1000 kg/m^3, P_0 as 10^5 Pa, gives

$$N \approx 3.47 \times 10^{-5} (w_{19.5})^3 \tag{10}$$

and it is seen that N is determined from the assumed function of air fraction of the seawater at the surface, $U(0)$, only. The earlier numerical process devised by Zinoviev et al. (10) gave $N \approx 3.55 \times 10^{-5} (w_{19.5})^3$, which is clearly close to Equation (10).

3.2 Determination of layer "thickness" *m* from physical parameters

As in the case of the layer "strength" parameter N, the earlier analysis of Zinoviev et al. (6, 10) included a numerical process by which the value of m was determined by matching the sound speed profile of the "Ainslie" bubbly layer to the sound speed profile of the "Brekhovkikh" transitional layer. As with parameter N, it was considered preferable to obtain a derivation of m based on the parameters of the bubble population model. This new analysis is described below.

Examples of the SSPs obtained for Brekhovskikh's transitional layer, where values of N and m were obtained by the numerical "best fit" process, are shown in Figure 3 for four values of wind speed. These SSPs are shown together with those obtained by application of the full analysis described by Ainslie (3), the latter being the profiles to which the values of N and m had been matched. A set of layer boundaries indicated in this figure were arbitrarily specified as occurring at the depth at which the sound speed gradient is triple that for an isothermal gradient, that is, where the gradient is 0.051 s^{-1}. It was considered that this was a reasonable means of defining a boundary for practical purposes.

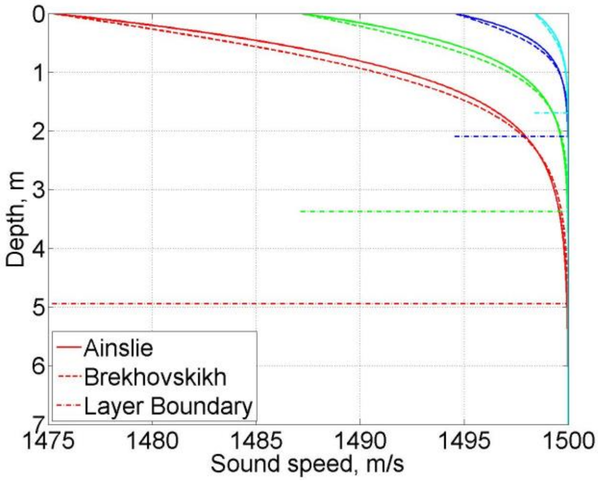

Figure 3 – Sound speed profiles for wind speeds $w_{19.5}$ 5, 7.5, 10, 12.5 m/s based on (i) full bubble analysis of Ainslie (3), (ii) parameters *N* and *m* matched to Brekhovskikh's transitional layer model (2). Depth of bubbly layer when gradient is 0.051 s^{-1} (dashed line).

The depth-dependent air fraction described by Ainslie (3) is $U(z) = U(0)\,[J(z)/J(0)]\exp\left(-z/L_{w_{19.5}}\right)$, which for depths relevant to these considerations may be shown to be adequately approximately as

$$U(z) \approx U(0)\exp\left(-z/L_{w_{19.5}}\right) \tag{11}$$

where $L_{w_{19.5}}$ is a wind speed dependent correlation depth, defined as [3]

$$\begin{aligned} L_{w_{19.5}} &= 0.4\,\text{m for}\, w_{19.5} \le 8\,\text{m/s} \\ &= 0.4 + 0.115[w_{19.5} - 8]\,\text{m for}\, w_{19.5} > 8\,\text{m/s}. \end{aligned} \tag{12}$$

Ainslie attributes the origin of the exponential term incorporating the correlation depth $L_{w_{19.5}}$ to the bubble population distribution of the Hall-Novarini model. By consideration of Equation (6), neglecting the depth dependence of $P(z)$, and substituting for $U(z)$ using the approximated form of Equation (11), it may be shown that $c(z)$ will approach its limiting value (c_0) at a depth such that $\exp\left(-z/L_{w_{19.5}}\right)$ becomes very small. Clearly, the key aspect of the bubble model in the determination of $c(z)$ is the assumption of an exponential decline of bubble fraction with depth, and the nomination of the depth correlation constant.

An estimate of *m* based on the physical parameters, may be made by matching the slopes of the two SSPs when the product mz becomes >>1. From the data in Figure 3, the slopes do appear well matched at locations which are deep in the bubbly layer.

Firstly, the slope of the SSP for Brekhovskikh's transitional layer may be obtained using Equation (3) and approximating for mz >>1. In this process, $e^{mz}/\left(1+e^{mz}\right)$ is replaced by $1 - 1/e^{mz}$, then further approximation using Taylor series terms gives

$$c(z)\big|_{mz \gg 1} \approx c_0\left(1 - \frac{N}{2e^{mz}} - \frac{N^2}{2}\right). \tag{13}$$

After differentiating with respect to *z*, and substituting for *N* in terms of surface air fraction using Equation (9), the sound speed gradient is

$$\left.\frac{d\,c(z)}{d\,z}\right|_{mz \gg 1} \approx \frac{\rho_0\, c_0{}^3\, U(0) m e^{-mz}}{P_0}\ \text{s}^{-1} \tag{14}$$

The sound speed gradient for the Ainslie bubble profile may be obtained using Equation (6). Here, the equation is re-formed in terms of $c(z)$, and then suitable Taylor series approximations are made. Next, substitution is made for the depth-dependent air fraction $U(z)$ using the simplified form of Equation (11), and after some re-arrangement, the sound speed gradient follows as

$$\frac{d\,c(z)}{d\,z} \approx \frac{\rho_0\, {c_0}^3\, U(0)\exp\left(-z/L_{w_{19.5}}\right)}{2\,P(z)}\left[\frac{1}{L_{w_{19.5}}}+\frac{\rho_0\, g}{P(z)}\right] \tag{15}$$

where $P_0+\rho_0\, g\, z$ may be substituted for $P(z)$, where P_0 is atmospheric pressure at the ocean surface and g is acceleration due to gravity, ms^{-2}.

If the sound speed gradients in Equations (14) and (15) are equated for a depth z equal to 4 times the wind speed-dependent correlation length $L_{w_{19.5}}$, the following expression may be obtained

$$\left(m\, L_{w_{19.5}}\right)\exp\left(-4\, m\, L_{w_{19.5}}\right) \approx \frac{e^{-4}\left(1+5\,\rho_0\, g\, L_{w_{19.5}}/P_0\right)}{2\left(1+4\,\rho_0\, g\, L_{w_{19.5}}/P_0\right)^2} \tag{16}$$

A consequence of equating Equations (14) and (15) is the cancellation of the terms $U(0)$. The solution for m is then influenced mainly by the value for the correlation depth $L_{w_{19.5}}$.

For wind speeds ≤ 8 m/s, for which $L_{w_{19.5}} = 0.4\,\mathrm{m}$, making substitutions for ρ_0, g and P_0 used earlier, it may be shown that $m \approx 3.147\ \mathrm{m}^{-1}$. Taking account of the variation of $L_{w_{19.5}}$ with wind speed indicated by Equation (12), the full solution from Equation (16) may be shown to be

$$\begin{aligned} m &= 3.147 && \text{if } w_{19.5} \le 8\,\mathrm{m/s} \\ &\approx \left(0.085 w_{19.5} - 0.35\right)^{-1} && \text{if } w_{19.5} > 8\,\mathrm{m/s}. \end{aligned} \tag{17}$$

These values of m, based on Equations (16), and ultimately on the bubble model, are close to those obtained early by Zinoviev et al. by numerical matching of the sound speed profile of the “Ainslie” bubbly layer to the sound speed profile of the “Brekhovkikh” transitional layer. That earlier determination gave $m \approx 3.10\ \mathrm{m}^{-1}$ for $w_{19.5} \le 8\,\mathrm{m/s}$ and $m \approx \left(0.079 w_{19.5} - 0.31\right)^{-1}\mathrm{m}^{-1}$ for $w_{19.5} > 8\,\mathrm{m/s}$.

4. SOLUTION FOR THE GRAZING ANGLE AT THE SURFACE

Brekhovskikh (2) showed that if a plane wave approaches the transitional layer from below, with the grazing angle β_0, between the bottom of the layer and the horizontal axis forming the surface, the solution for the acoustic pressure of the incident acoustic wave as it advances within the layer can be written with the use of hypergeometric series. By applying Brekhovskikh’s solution for the acoustic pressure to the transitional layer, Zinoviev et al. (6, 10) derived a complex system of equations for determining the grazing angle, β_s, of the energy density vector at the surface. This analysis determined that the series summations required to obtain β_s were dependent the incident angle β_0 below the layer, the sound speed c_0 below the layer, plus two parameters δ and μ, as follows:

$$\delta = \frac{2\pi f}{m c_0}\left[\sin\beta_0\right], \text{ non-dimensional} \tag{18}$$

$$\mu = \frac{2\pi f \sqrt{N}}{m\, c_0 \sqrt{1-N}} \approx \frac{2\pi f}{m\, c_0}\sqrt{N} \quad \text{as } N \text{ is small, non-dimensional} \tag{19}$$

The values of N and m may now be substituted in terms of the physical parameters of the bubble model, in particular, substituting for N from Equation (10) and for m from Equation (17) gives

$$\begin{aligned} \mu &\approx 7.84\times10^{-6}\, f\, {w_{19.5}}^{3/2} && \text{if } w_{19.5} \le 8\,\mathrm{m/s} \\ &\approx 2.47\times10^{-5}\left[0.085 w_{19.5} - 0.35\right] f\, {w_{19.5}}^{3/2} && \text{if } w_{19.5} > 8\,\mathrm{m/s}. \end{aligned} \tag{20}$$

4.1 Approximate solution for the grazing angle at the surface

In Equation (19), μ has the form of a non-dimensional frequency *f*. From Equation (18), $\delta \approx 2\pi\, f\, \beta_0 / (m\, c_0)$ for small β_0, and δ may be considered to be a parameter in place of β_0. The grazing angle at the surface β_s may then be considered as a function of μ and δ, only, as they incorporate frequency *f* and incident angle β_0. Assuming that values of *m* do not vary greatly, which is borne out by values that may be determined from Equation (17), $\beta_s \approx f_a(\mu,\delta) \approx f_b(\mu,\beta_0)$ where β_0 is considered to be small. Using Taylor series expansions in terms of each of μ and β_0, considering now the resulting series for a particular value of μ, we may express β_s in terms of functions of μ, such as $g_0(\mu)$, $g_1(\mu)$, $g_2(\mu)$, …, as

$$\beta_s \approx g_0(\mu) + \beta_0\, g_1(\mu) + {\beta_0}^2 g_2(\mu) + \ldots \tag{21}$$

Evaluation of the full function for β_s in terms of μ and β_0 shows that β_s is always zero when β_0 is zero, so it follows that $g_0(\mu) = 0$ in Equation (21). By further consideration of examples of the full solution, it is observed that β_s is a linear function of β_0 for very small values of β_0, so that terms in ${\beta_0}^2$ and higher powers may be assumed neglected for this approximate solution, hence $\beta_s|_{\beta_0 \to 0} \approx \beta_0\, g_1(\mu)$. If μ is assumed < 1.0, a Taylor series expansion of function $\beta_0\, g_1(\mu)$ then gives

$$\beta_s|_{\beta_0 \to 0} \approx \beta_0\left(f_0 + \mu\, f_1 + \mu^2\, f_2 \ldots + \mu^n\, f_n\right) \tag{22}$$

and it can be assumed that β_s may be expressed as β_0 multiplied by a polynominal function in μ, for small β_0. Zinoviev (10) obtained a partial analytic solution for β_s, in which the full function for β_s was expected to lie between $\beta_0\left(1 + 1.19\mu^2\right)$ and $\beta_0\left(1 + 1.96\mu^2\right)$. Here, there was an expectation that the next term in a more complete solution was 4th order in μ, and so it was presumed that $\mu^4 < 0.1$, approximately, was a requirement for this solution. Tests showed that μ^4 needed to be considerably smaller than 0.1 to use this solution, and by inspection of Equation (20) the relevant wind speed and frequency combinations were constrained to modest surface roughness. For higher roughness levels, the full Brekhovskikh solution is still expected to converge to a relationship between β_s in terms of β_0 and μ for very small β_0, as in Equation (22) convergence is expected for $\mu < 1$, although it may not be practical to determine an analytic solution. For this reason, the function $f(\beta_0, \mu) = \beta_s$ was estimated numerically, based on values of β_s determined in terms of β_0 and μ from the full Brekhovskikh solution, for β_0 near 0.0. Including terms in μ to the power 6, this function was found to be

$$\beta_s \approx \beta_0\left(1 + 1.95\mu^2 - 0.4\mu^4 + 4.9\mu^6\right). \tag{23}$$

This expression was determined from data within frequency values of 1 kHz and 9 kHz, and for wind speeds covering both modest and large roughness values with $\mu < 1$.

4.2 Snell's Law Solution

The surface grazing angle β_s obtained using the full Brekhovskikh solution may be shown to approach the Snell's law result in both the high frequency limit and the limit of steep incidence angle β_0. The analysis in section 4.1 is not relevant under these conditions as (i) high frequency implies that $\mu \gg 1$, (ii) large incidence angle violates the assumptions for Equation (22). When Snell's law applies, the angle of incidence at the surface is exactly $\beta_s = \arccos\left(c_s \cos\beta_0 / c_0\right)$. If c_Δ is the change in surface sound speed caused by the bubbles, Snell's law leads to the approximation

$$\beta_s \approx \sqrt{2 c_\Delta / c_0 + {\beta_0}^2} \tag{24}$$

and as c_Δ is finite, β_s is not zero even if the incident grazing angle β_0 approaches zero.

4.3 Example of Surface Incidence Approximation

Figure 4 shows the surface grazing angle β_s as a function of the incidence angle β_0 below the bubbly region for two wind speed-frequency examples for which μ^4 is 0.3 (for which $\mu = 0.740$). These results are typical of those for other wind speed-frequency combinations for which μ^4 is as large as 0.5. Here, the value of $\mu = 0.740$ was determined using values for N and m which were obtained from the numerical matching to the sound speed profile described by the full analysis of Ainslie. This was done in order to test the use of the simplified analysis, in which μ is obtained from Equation (20) and β_s from Equation (23).

The full Brekhovskikh solution, shown by the red curve, approximates a near-linear function in β_0 for small angles, and approaches the Snell's law solution at steeper incident angles β_0 as expected. The green line represents the case for which the bubbly layer is absent, for which there is no change in angle. The difference between the green line and the full solution in red illustrates the change in angle caused by the thin layer of sound speed change. It is also clear that Snell's law is not correct for small incidence angles β_0. The analytic function, shown by the two cyan curves, is not accurate for this value of μ^4, as was expected. In Figure 4 (a), the dashed line, obtained by computing a value of $\mu \approx 0.7535$ using Equation (20), then substituting into Equation (23) to obtain $\beta_s \approx 2.87\beta_0$, clearly adheres to the full Brekhovskikh solution for very small values of incident angle β_0. For Figure 4 (b) the corresponding value of μ is 0.7315, giving $\beta_s \approx 2.68\beta_0$ and again the dashed line is very close to the full Brekhovskikh solution for very small values of β_0

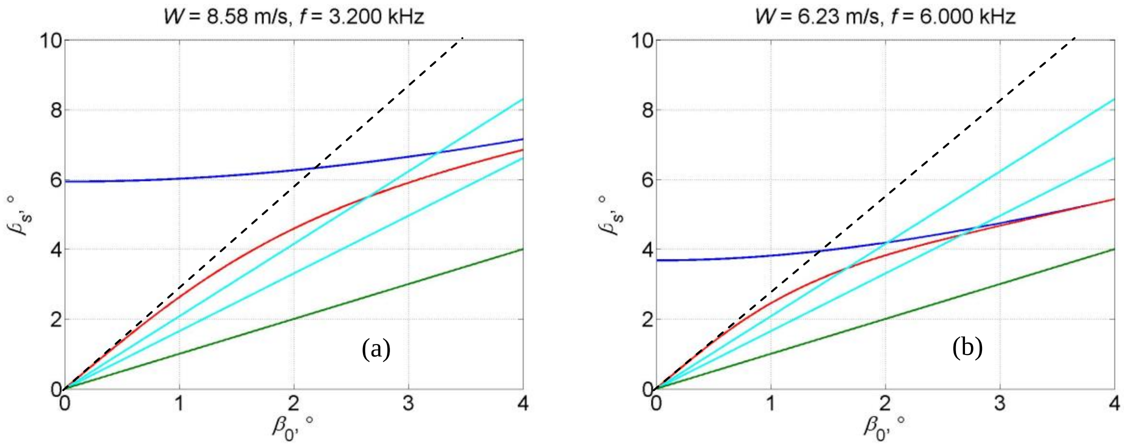

Figure 4 – Grazing angle β_s at surface as function of incident angle below layer β_0 for $\mu^4 = 0.3$, (a) $w_{19.5} = 8.58$ m/s, $f = 3.2$ kHz, (b) $w_{19.5} = 6.23$ m/s, $f = 6$ kHz. Top and bottom cyan lines - $\beta_0(1+1.96\mu^2)$ and $\beta_0(1+1.19\mu^2)$ respectively, red line – full solution for Brekhovskikh transitional layer, dotted line – Equation (23), green line – no layer, blue line – exact Snell's law.

The approximation that has been adopted for the simplified JBZ model is to take as surface grazing angle β_s the lesser of the value from the uniform slope approximation (Equation (23)) and the Snell's law solution. This nature of the error, relative to the full solution, is worth some consideration.

From Equation (20), μ incorporates the term $f\,w_{19.5}^{3/2}$, so for a given value of μ, if frequency is low, wind speed is high, and vice versa. Now, from Equation (24), substituting for c_Δ in terms of N using Equation (5), and for N using Equation (10), for an incident angle $\beta_0 \to 0$, it follows that $\beta_s|_{\beta_0 \to 0} \approx 4.2\times10^{-3}(w_{19.5})^{3/2}$.

Hence, for a given value of μ, a higher frequency will be associated with a lower wind speed and the Snell's law curve on Figure 4 will appear to be shifted to lower angles β_s. The slope of the full Brekhovskikh solution at small angles, approximated by Equation (23), is unchanged for a given μ, and so the full solution approaches Snell's law at smaller values of incidence angle β_0. The angle β_0 at which the Snell's law solution is approached is reduced, ensuring a good fit for that value β_0 and greater, as seen in Figure 4 (b). For lower frequencies, the Snell's law curve will be shifted to larger values of β_s and the full Brekhovskikh solution will approach Snell' law at a larger value β_0. However, this extends the span of small values of β_0 for which the linear result approaches the full Brekhovskikh solution. Thus it appears that taking the lesser of the value from Equation (23) and the full Snell's law solution as β_s will be adequate for any frequency/wind speed combination.

5. DEMONSTRATION OF APPROXIMATE SOLUTION

A demonstration of the use of the full JBZ model, run with a Gaussian beam transmission model, had been presented by Jones et al. (7). Work of this type has now been repeated using the simplified JBZ model of surface reflection loss as outlined in section 2. Here, simulations of *TL* versus range were carried out for a surface ducted scenario - an isothermal surface duct of depth 64 m over an infinitely deep, isovelocity ocean, with sound source and receiver at 18 m depth. *TL* effects may then be attributed solely to sound travelling within the surface duct. The Gaussian beam model was run, firstly, with the simplified JBZ model describing surface reflection loss, and then, for comparison, with Beckmann-Spizzichino (B-S) surface reflection loss model described by Hodges (11). Runs of the Gaussian beam model were also made with the surface loss fixed at zero, to simulate a smooth surface. In all cases, the summation of multi-path energy was incoherent. Values of the component of *TL* due to coherent surface reflection loss, labelled ΔTL_{cTL}, were obtained as a function of range by subtracting corresponding values of smooth-surface *TL* from with-wind *TL* data. These derived values of ΔTL_{cTL} are compared with the data from the use of the B-S model, in Figure 5.

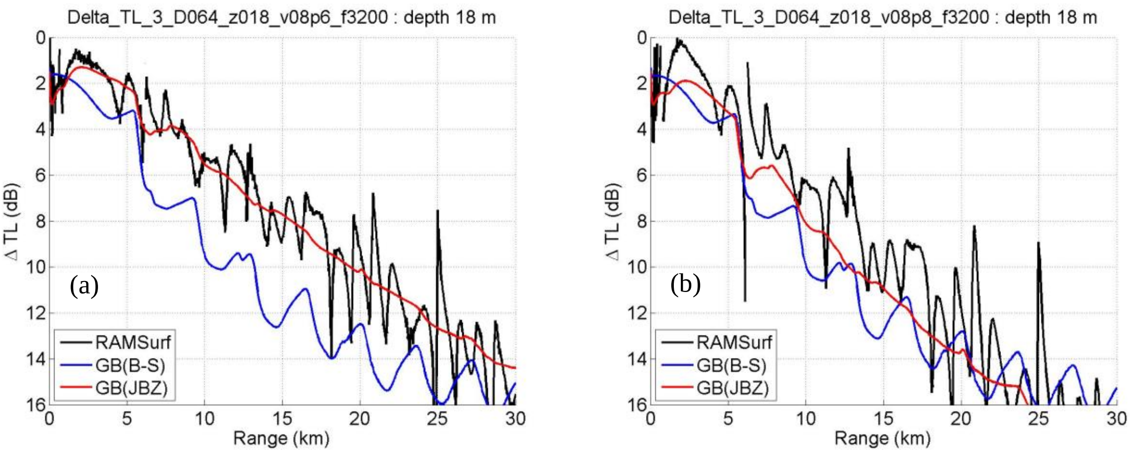

Figure 5 – Loss due to coherent surface reflection loss (ΔTL_{cTL}), RAMSurf (black), Gaussian beam model with simplified JBZ (red), Gaussian beam model with B-S (blue), source & receiver at 18 m, (a) $w_{19.5}$ = 8.6 m/s, f = 3.2 kHz (μ^4 = 0.31), (b) $w_{19.5}$ = 8.8 m/s, f = 3.2 kHz (μ^4 = 0.42).

Also shown are values of ΔTL_{cTL} derived from Monte Carlo runs of the RAMSurf PE code (12) for the same scenarios. As described briefly by Jones et al. (7), for each scenario RAMSurf included the sound speed variation due to wind-induced bubbles added to the isothermal variation. Here, Ainslie's full model of sound speed variation (3) was used. RAMSurf was used to compute the coherent pressure field, in range r and depth z, for each of a large number (typically 40) of Monte Carlo realisations of the rough surface in accordance with the appropriate spectrum of surface waves. The mean received coherent pressure field was obtained by coherent averaging of the pressure values at all grid points in range and depth. For each scenario, RAMSurf was also run with the effects of wind removed, that is, with a smooth sea surface and with an isothermal sound speed variation, only, in the surface duct. The coherent loss due to surface loss was obtained by subtracting the smooth surface *TL* from the wind-roughened surface *TL*.

5.1 Discussion

The data shown in Figure 4 (a) are relevant to the values of ΔTL_{cTL} shown in Figure 5 (a). Now, for an isothermal surface duct of thickness 64 m, the angle of surface incidence for a limiting ray may be shown to be about 2.2°. For this isothermal duct overlaid by a wind-induced bubble region of about 3 m thickness, the incidence angle β_0 for sound at the base of the bubbly region will be almost the same, about 2.2°. There will, of course, be incident rays for which the turning point is above the base of the duct, and for which the incidence angle will be < 2.2°. From Figure 4 (a) it may be seen that the values of β_s returned by the full Brekhovskikh solution will be slightly less than those from the approximate solution. The impact on ΔTL_{cTL} obtained using the simplified JBZ appears to be insignificant, as the values obtained using it with the Gaussian beam model, the red curve, agree very well with those obtained by the RAMSurf modelling. The corresponding B-S data are not as close.

The data in Figure 5 (b) again show good agreement obtained by using the simplified JBZ model, for this example with higher surface roughness, for which $\mu^4 = 0.42$.

6. CONCLUSIONS

A significant simplification has been made to the JBZ model of coherent surface loss for application to forward transmission of underwater sound in scenarios involving small angles of incidence at a wind-roughened surface incorporating near-surface bubbles. The simplified JBZ model includes an approximation to the angle of surface incidence and an approximation to the second-order small-slope model of surface roughness loss, that appear adequate for any angle of below-bubble layer sound incidence including very small angles. The determination of surface incidence angle appears to be largely related to the bubble-related air fraction at the surface and the assumed rate of change of air fraction with depth. The simplified JBZ model has been verified to a limited degree by comparison with data obtained from Monte Carlo runs of RAMSurf in simulation of wind-roughened ocean scenarios which include the effects of near-surface bubbles on sound speed. The roughness situations for which the simplified JBZ model appears adequate are expressed in terms of a parameter incorporating a product of wind speed to the power 1.5 and acoustic frequency.

REFERENCES

1. Jones AD, Duncan AJ, Bartel DW, Zinoviev A & Maggi A. Recent Developments in Modelling Acoustic Reflection Loss at the Rough Ocean Surface. Proc Acoustics 2011; Gold Coast, Australia 2011.
2. Brekhovskikh LM. Waves in Layered Media. New York: Academic Press; 1960.
3. Ainslie MA. Effect of wind-generated bubbles on fixed range acoustic attenuation in shallow water at 1 – 4 kHz. J Acoust Soc Am. 2005; 118: 3513–3523.
4. Hall MV. A comprehensive model of wind-generated bubbles in the ocean and predictions of the effects on sound propagation at frequencies up to 40 kHz. J Acoust Soc Am. 1989; 86(3): 1103-17.
5. Keiffer RS, Novarini JC, Norton GV. The impact of the background bubble layer on reverberation-derived scattering strengths in the low to moderate frequency range. J Acoust Soc Am. 1995; 97(1): 227-34
6. Zinoviev A, Bartel DW, Jones AD. An Investigation of Plane Wave Propagation through a Layer with High Sound Speed Gradient. Proc Acoustics 2012; Fremantle, Australia 2012.
7. Jones AD, Duncan AJ, Bartel DW, Zinoviev A, Maggi AL. A Physics-Based Model of Surface Reflection Loss for Ray Models. Proc 11th European Conference on Underwater Acoustics; 2–6 July 2012; Edinburgh, UK 2012. p. 77–84.
8. Jones AD, Zinoviev A, Bartel DW. Approximation of a physics-based model of surface reflection loss. J Acoust Soc Am. 2014; 135: 2300.
9. Williams KL, Thorsos EI, Elam WT. Examination of coherent surface reflection coefficient (CSRC) approximations in shallow water propagation. J Acoust Soc Am. 2004; 116(4): 1975–1984.
10. Zinoviev A, Jones AD. Approximate solutions for an acoustic plane wave propagation in a layer with high sound speed gradient. Proc Acoustics 2013 – Victor Harbor; 17-20 November 2013; Victor Harbor, Australia 2013.
11. Hodges RP. Underwater Acoustics: Analysis, Design and Performance of Sonar. John Wiley & Sons Ltd.; 2010. p. 106-108.
12. Ocean Acoustics Library (US), supported by Office of Naval Research (US). Available from: http://oalib.hlsresearch.com/PE/ramsurf/. RAMSurf version 1.5.f was used in this work.